Collagen imaged by Coherent X-ray Diffraction: towards a complementary tool to conventional scanning SAXS

2010 J. Phys.: Conf. Ser. 247 012004

(http://iopscience.iop.org/1742-6596/247/1/012004)

Collagen imaged by Coherent X-ray Diffraction: towards a complementary tool to conventional scanning SAXS

Felisa Berenguer de la Cuesta[1,*], Richard J Bean[1], Catriona McCallion[2], Kris Wallace[2], Laurent Bozec[1, 3], Jen C Hiller[4], Nicholas J Terrill[4], Ian K Robinson[1,4]

1 London Centre for Nanotechnology (LCN), University College London (UCL), London WC1H 0AH, United Kingdom

2 Department of Physics and Astronomy, University College London (UCL), London WC1E 6BT, United Kingdom

3 Biomaterials and Tissue Engineering, Eastman Dental Institute, UCL, London WC1X 8LD, United Kingdom

4 Diamond Light Source, Harwell Science and Innovation Campus, Didcot, Oxfordshire OX11 0DE, United Kingdom

Corresponding author e-mail address: f.berenguer@ucl.ac.uk

Abstract. Third generation x-ray sources offer unique possibilities for exploiting coherence in the study of materials. New insights in the structure and dynamics of soft condensed matter and biological samples can be obtained by coherent x-ray diffraction (CXD). However, the experimental procedures for applying these methods to collagen tissues are still under development. We present here an investigation for the optimal procedure in order to obtain high quality CXD data from collagen tissues. Sample handling and preparation and adequate coherence defining apertures are among the more relevant factors to take into account. The impact of the results is also discussed, in particular in comparison with the information that can be extracted from conventional scanning small angle x-ray scattering (SAXS). Images of collagen tissues obtained by CXD reconstructions will give additional information about the local structure with higher resolution and will complement scanning SAXS images.

1. Introduction

Small Angle X-ray Scattering (SAXS) has been traditionally applied to the study of a large range of biomaterials, from protein solutions to fibres and composites, as well as biological tissues such as muscle and bone. SAXS provides valuable information about the mesoscale of these systems, in particular over the range of a few tens of nanometers. However, the structural information in the sample is averaged over an area of typically 200-300 microns due to the size of the beam used. While some studies do not require a higher spatial resolution, in the case of biological tissues (that are highly hierarchical structures) the possibility of reducing the spot size together with the resolution is very appealing.

The introduction of microbeam facilities in SAXS beamlines [1] was a first step towards exploiting SAXS as an imaging technique for biomaterials. The use of microbeams in scanning and/or tomographic setups has opened a new range of possibilities in the study of tissues and fibres, with beam spot sizes of typically 3-50 microns [2]. Currently this technique is widely used in the study of biomaterials, for instance, in bone structure and micromechanics [3], soft tissue and cornea [4], natural polymers structure [5], or parchment and ancient materials [6]. With the advent of nanobeams in some facilities, such as ID13 at the European Synchrotron Radiation Facility (ESRF), we can expect new possibilities in the study of local structure, although the effects of the radiation damage induced by the highly intense focused nanobeams will be a relevant issue in soft matter samples.

The natural step further is to fully exploit the coherence of 3rd generation sources, together with micro or nano beam sizes, in order to extract as much information as possible from each exposure of the sample, therefore limiting the onset of radiation damage. When using a fully coherent beam, the scattered amplitudes of different areas of the sample interfere coherently, and the resulting diffracting pattern is proportional to the square of the sum of these amplitudes. On the other hand, if the incident beam is incoherent, the resulting diffraction pattern will be proportional to the sum of the intensities of the scattered waves from the different regions of the sample. Therefore, it is clear that a diffraction pattern from a coherent beam contains additional information about the sample nano and microstructure which is masked otherwise if the incident beam is incoherent. The extra information appears as speckles, or modulations of the intensity distribution and can be used by phase retrieval algorithms [7-10] in order to recover the amplitude and phase transmission functions of the sample with a resolution (ideally) only limited by the wavelength. This information can be combined with the results from scanning microbeam SAXS and/or tomography SAXS to get a more complete picture of the sample structure.

We are particularly interested in the applications of Coherent X-ray Diffraction (CXD) to collagen tissues in the small angle regime, in particular tendon and bone. In the case of bone, current non-coherent scanning SAXS can give relevant information about the location and orientation of the mineral phase [3], in some cases with 1 micron spatial resolution. However, in order to study the osteogenesis and mineralization processes it would be very interesting to obtain similar information, with improved resolution, about the disposition and orientation of the organic matrix of collagen fibres. Some recent studies using scanning SAXS in tendon samples show promising results [4] although the spatial resolution is still unsatisfactory (20 microns). In the present paper, we present CXD methods, in particular ptychography, as a potential and powerful complementary method that may be used for obtained dark field images of collagen tissues with a resolution of some tens of nanometers.

2. Coherent X-ray Diffraction

Coherent X-ray Diffraction imaging is based on the inversion of speckled far-field diffraction patterns in order to obtain the complex-valued (amplitude and phase) transmission function of the sample. This so-called inversion process involves, as a first step, the retrieval of the phases on the detector plane of the diffracted waves using iterative phasing algorithms. This is achieved using the intensities recorded in the diffraction patterns together with some constraints imposed from the sample transmission function, the illuminating wavefront, or both. Once the amplitude and phase of the diffracted wave has been determined on the detector plane the next step is a propagation of the wave back to the sample exit plane (done usually by calculating the wave inverse Fourier transform) to obtain the sample complex-valued transmission function. CXD inversion algorithms require the patterns to be oversampled [11], so the maximum spatial frequency in the pattern is at least two times bigger than the detector pixel size. In most cases, this is achieved by illuminating a small isolated sample under a fully coherent beam, so that all the density of the object is contained in a delimited region of the beam footprint, whereas the sample density outside this area is 0. This fact can be translated onto a mathematical real-space constraint in most part of the CXD phasing algorithms, as one requires that

the density of the reconstructed sample is contained in a portion (the so-called "support") of the total area covered by the beam. The use of this real-space constraint in the inversion process has proven to be a successful approach in a range of problems both in material science [12] and biology [13]. However, the requirement for a small isolated object being smaller than the beam footprint constitutes a limitation for a wide range of scientific cases. In the past few years several new approaches have proposed tackling the inversion problem from alternative perspectives; namely ptychography, "keyhole" diffractive imaging and wavefront modulation-based imaging.

Ptychography is based on a different approach to the inversion process of a series of diffraction patterns, each one recorded from different illuminated areas in the sample [8]. A given amount of overlap (ideally a minimum of ~60% [14]) is required between different illuminated areas. Here the redundant information in successive patterns gives a strong constraint to the inversion algorithm. An efficient first ptychography algorithm was presented by Rodenburg and Faulkner [8] and demonstrated for x-rays shortly afterwards [15]. However, the first algorithms required an extremely good knowledge of the probe wavefront profile in order to obtain a good convergence. This limitation has been overcome recently by Thibault and colleagues [9], where they demonstrated that both the sample transmission function (amplitude and phase) and the probe wavefront profile can be obtained from the same ptychography dataset. Other recent methods [10] also reconstruct the illumination function. This set of ptychography algorithms has proved to be powerful in the reconstruction of some relevant samples not only with visible light [10] but also in the case of hard x-rays [16] and electrons [17]. In all these cases, the data were obtained in a forward scattering geometry; ptychography has not yet been proved to work under Bragg diffraction. Although the use of the latest algorithms that reconstruct also the illuminating wavefield has eased the inversion problem, the technique is still quite sensitive to errors in the probe position, effects due to partial coherence in the beam and poor signal-to-noise ratio.

The phase retrieval process in both conventional "support"-based methods and ptychography evolves by Fourier transformations of the scattered waves between real and reciprocal spaces in two planes: the one of the sample and the one of the detector, where the diffraction patterns are recorded. When using the information from a third plane, additional constraints are added to the iterative process and the reconstruction of the sample transmission function is in principle improved. Both keyhole coherent diffraction and wavefront modulation-based methods are rooted in this idea. Keyhole coherent diffractive imaging has been demonstrated recently [18]. It uses a curved illumination and solves initially for the illumination wavefront and then, in a second step, the sample transmission function [19]. The method is powerful although it is sensitive to errors in the optical elements distances determination.

Another interesting possibility is to introduce a known phase modulator downstream of the sample [20]. Here a set of diffraction patterns are recorded for different transverse positions of the phase modulator, illuminating the same area of the sample. The method has been demonstrated for visible light [21] and hard x-rays [22] and nicely overcomes some of the requirements in the probe characteristics and signal-to-noise ratio needed in other CXD methods such as ptychography and keyhole imaging. However, the fact that the same area of the sample is illuminated during the modulator scan might induce the onset of radiation damage in the case of some biological samples, which could be delayed when scanning the sample instead (as done in ptychography).

In the present paper, we focus on the possibilities of Coherent X-ray Diffraction (in particular ptychography) for the imaging of biological specimens as a complementary tool to conventional scanning SAXS, providing extra information that could not be accessible otherwise. The technique has already been successful in obtaining images of biosamples such as bacteria [16] and blood cells [23]. However, we are interested in extending ptychography to the Bragg diffraction geometry. In such a way, the technique could be used for obtaining dark field images of biological extended samples, in particular collagen [24] or cellulose-based tissues. Here dark field is used to describe the diffraction contrast of the different components of the sample which can be exploited in order to obtain images where only the distribution of one single component (the one from which the Bragg reflections have been used for the CXD reconstruction process) is visible, whereas all the other components are

filtered. This is attractive, for example, in the study of composite materials or biological tissues, as we can obtain images with the distribution of each one of the components separately. When imaging materials where the different components show small differences in terms of absorption and phase contrast, the ability to exploit the diffraction contrast provided by dark field ptychography can be useful. Our motivation here was to study the experimental requirements needed in Bragg diffraction ptychography of collagen tissues taking into account the more or less value of the output information that may be obtained from a given sample reconstruction.

3. Materials and methods

Samples consisted of collagen fibres carefully extracted from rat tail tendons [25]. The tails, from young adult healthy rats, were kept frozen until dissection. The dissection involved a careful extraction of the four tendons of the tail after skin removal. This operation is difficult as tendons are strongly attached to the tiny bones of the tail and needs to be done by means of short, quick and precise stroke movements of the dissection tweezers; otherwise the superficial part of the tendon is damaged. We carefully removed the blood vessels and connective tissue attached to the tendons. Collagen fibres of ca. 10 mm long and about 0.3-0.5 mm diameter were extracted simply by pulling them from the central part of the tendon in saline solution and mounted slightly stretched in a suitable cell filled with phosphate buffer solution (7.4 pH). The cell is a brass cell specially designed to clamp the fibres keeping them parallel without introducing additional stretching. It has a reservoir for buffer solution and two mica windows (each 25 μm thick) with a total x-ray path length of 2 mm. The scatter from the solution volume was found to be relevant close to the beamstop, but had less affect in the Q-range of interest for this experiment (around 0.009 A^{-1}). In this way the samples were kept wet during the data acquisition. This increased the useful lifetime of the samples exposed to the beam, as the liquid reduced the heat load on the collagen fibres and hence the radiation damage produced by thermal denaturalization of collagen. Although the presence of liquid accelerates the other mechanisms of radiation damage in collagen, such as hydrogen bonds dissociation, which are firstly noticeable as a lost of intensity in the highest orders of diffraction, here we were concerned only about the first meridional reflection preservation. This peak is rapidly affected by the process of thermal denaturalization, so the presence of buffer solution greatly helps us to record diffraction patterns with 120 sec exposure time before the effects of radiation damage were noticeable.

Data were collected in three runs at beamline I22, Diamond Light Source (UK). The beamline is fed by an IV-25 undulator. The double crystal fixed exit Si (111) monochromator offers an energy resolution of 10^{-4} and the beamline uses a pair of Kirkpatrick-Baez mirrors for focusing and harmonics rejection. The beam energy was set to 8.5 keV, corresponding to a wavelength λ of about 0.1459 nm. An optically-coupled CCD camera (PI-SCX 1300 from Princeton Instruments, with 1340 x 1300 pixels, pixel size 20 microns, 16-bites dynamic range) was mounted at a distance of 5.2-5.7 m (depending on the experiment) from the sample in order to cover the Q-range of interest (0.006 to 0.011 A^{-1}). The distance sample-to-detector matters in a CXD experiment in the small angle regime as it is linked to the resolution of the reconstruction given by the algorithm as well as to the defining coherence aperture-to-detector distance. The former defines the size of the speckles observed on the detector and needs to be adjusted so the speckles are oversampled (at least 2 CCD pixels per speckle) [11] and hence make possible the use of iterative phase retrieval algorithms for reconstructing the sample.

We used two different configurations for the coherence defining aperture. In a first setup, the aperture was a square of 25 x 25 μm^2 defined by a pair of slits at 1.4 m upstream the sample. The last set of slits in the beamline, located at 0.4 m in front of the sample, was used as guard slits. Because of partial coherence effects observed (see Results section) we used a set of 2 pinholes and modified distances between the elements for the most recent run. The first pinhole (20 μm) was located at 11 cm upstream from the sample, followed by a second 100 μm pinhole at 3 cm for removing parasitic

scattering. Each sample was measured in a set of overlapping positions spaced 2 μm, 3μm or 4μm apart, depending on the experiment.

4. Results

Figure 1 shows a typical diffraction pattern from the collagen fibres in one position of the ptychography scan. Because of the long distance between the sample and the CCD detector, only the first meridional orders of collagen (corresponding to a spacing of approximately 1/67 nm^{-1}, Q = 0.009 A^{-1}) are recorded. Based on experience of macroscopic rat-tail collagen samples, we would expect these reflections to form an arc with an angular size related to the degree of axial disorder of the fibrils within our sample [26]. However, in our data the reflections can be seen to form straight lines, which indicate that the fibrils are almost parallel, with a high degree of axial order in the tissue (compare figures 1a and 1b). Not all samples showed this phenomenon, but it was our impression that it represented our "best" samples, those which had undergone the least mechanical handling during preparation. The reflections are now confined in a smaller area of the diffraction pattern, hence reducing the intensity spread and increasing the signal-to-noise ratio of the Bragg peaks of interest. This is particularly relevant for us as the phase retrieval algorithms usually require strong measured intensities, and it was achieved thanks to an improved sample preparation protocol. In our previous work [24] the signal-to-noise ratio of the obtained diffraction patterns was low; hence phase retrieval algorithms could not be applied straightforwardly. It was evident that an investigation of the requirements for the data acquisition process was needed, in particular regarding the sample preparation protocols and the maximization of the beams natural coherence.

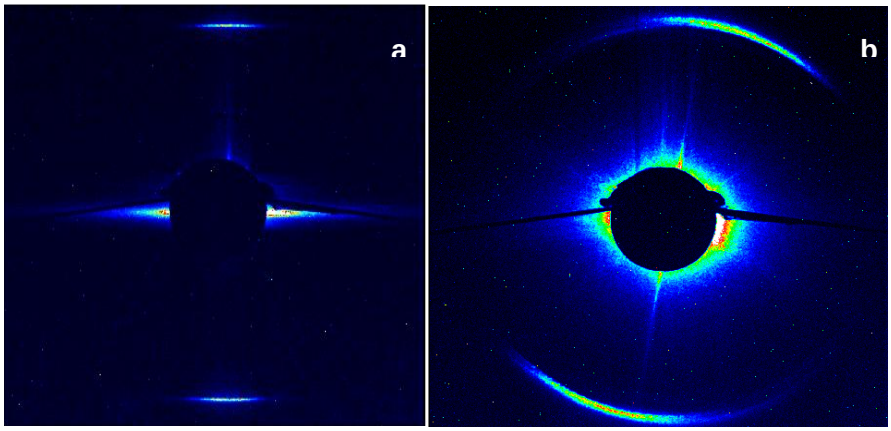

Figure 1. Diffraction patterns from different sections of the same rat tail tendon. For figure a) an accurate protocol for the sample preparation and handling was followed. The protocol included keeping the sample immersed in phosphate buffer solution at all times (see text). For b) this protocol was not followed and the handling process introduced a high degree of axial disorder in the fibrils distribution of the sample, as appreciated by the high azimuthal angle of the first meridional orders of collagen.

Another interesting fact is that the FWHM of the entire envelope of the Bragg peak along a raster line is ca. 100-200 pixels (with some sample-to-sample variation). This corresponds to a 0.3-0.6 μm width in real space of the diffracting motif, in this case, the fibrils within our sample. This value nicely fits with the typical diameter size of the fibrils expected in rat tail tendon. Obviously this approach is

only valid in the case where the motifs (fibrils) can be modeled as an array of cylinders with almost identical diameter and negligible axial disorder. We are confident that we can apply this model for data sets as the one in figure 1a as the reflections are almost straight lines.

The peaks show a rich speckled structure, easily noticeable in the zooms in figure 2. This is due to the spatial coherence in the illuminating beam, as we reported previously [24]. In the data set where a set of slits was used as coherence defining aperture, the first order reflections contain around 20-30 speckles of ca. 45-50 μm size (around 2.5 pixels in the CCD), corresponding to a square aperture of 25 x 25 μm^2 at a 7 m distance from the detector, as derived from the optical "grating" formula:

$$s = \frac{\lambda \cdot D}{d} \qquad \text{(eq. 1)}$$

where s is the speckle size, D is the aperture-detector distance, d the aperture size and λ the wavelength. Speckles of similar size could be observed when the defining aperture was a 20 μm pinhole at a distance of 7 m from the detector. This simple experiment shows that equation 1 is a good approximation for calculating the expected speckle size in coherent diffraction. Note that a good oversampling is achieved: the speckles are bigger than 2 CCD pixels, which is considered the minimum required in order to retrieve the phases by iterative algorithms [11].

A good estimate of the degree of coherence in the beam is the speckle visibility (in 1D) or speckle contrast (in 2D). The visibility can be calculated as the ratio (from the type of Young's double slit experiment described in [27]):

$$V = \frac{I_{\max} - I_{\min}}{I_{\max} + I_{\min}} \qquad \text{(eq. 2)}$$

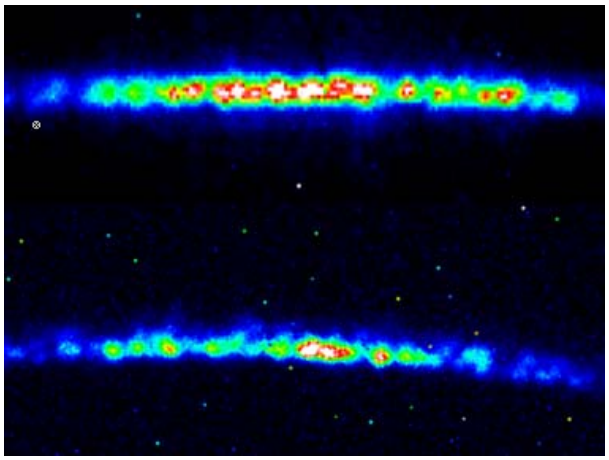

Figure 2. Zoom of the first meridional reflection of rat tail tendon fibres. The upper panel was obtained with the first setup, using a 25 x 25 μm^2 slit aperture. The bottom panel corresponds to the most recent setup with a 20 μm pinhole as the coherence-defining aperture. The contrast of the speckles is slightly better in the second setup (see text) although the small difference is not clearly appreciable in the 2D data. The upper pattern is more "one-dimensional" in the sense that it has less up-down variation in the speckle positions.

Figures 3a and 3b show the intensity of the central raster line through the first Bragg peak of two patterns for the 25 μm^2 slit aperture and the 20 μm pinhole, respectively. The visibility, as defined by equation 2, for the first case varies between 40% and 50% from sample to sample and with the total exposure time (this is an indicator of radiation damage starting to appear). However, for the more recent setup with the pinhole, the visibility increases to ~50-57% depending on the sample under investigation. There are several factors contributing to this difference: firstly, both measurements were made with samples from different specimens, so we should expect a small variation in the visibility due to this fact. Also, there is some loss of contrast inherent to the sample: simple simulations of the sample as a 3D array of cylinders with a distribution of different diameters predict a minimum

visibility of at least 20%. Finally, the buffer solution contributes to the incoherent scattered intensity in each peak, thus increasing the I_{min} recorded and effectively reducing the visibility.

There are also other factors than the ones directly related to the sample nature and characteristics, in particular the degree of coherence in the beam notably affects the visibility of the speckles in CXD studies. If there is any incoherent part of the beam, it will give rise to the smooth part of the Bragg peak underneath the speckles. In the limiting case where the beam is totally incoherent, the speckles will not appear and the Bragg peak will be constituted simply by the smooth intensity distribution. In the opposite case, a fully coherent beam will give (ideally) a speckled pattern with up to 100% contrast, that is, which means an intensity value reaching zero between speckles. In our experiments, the dimensions of the pinhole (20 μm) are within the transverse coherence length values expected for the beamline. The 25 μm^2 slit aperture is close to the limit, so a great loss of visibility and speckle contrast should be expected for this case, as shown in figure 3.

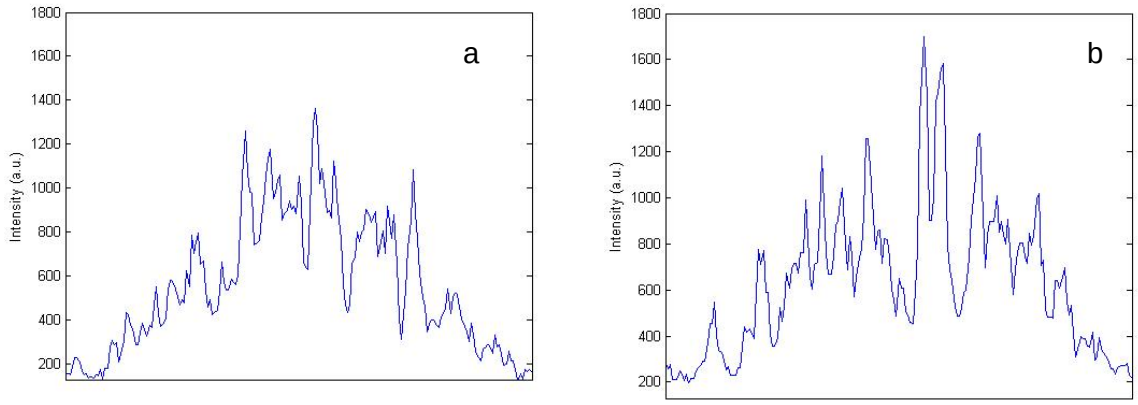

Figure 3. One dimensional profiles of the first order Bragg peak of rat tail tendon for 2 different defining coherent apertures. In a), we used 25 x 25 μm^2 slits; in b) a 20 μm pinhole. The visibility is greater in the second case. Note that some variation of the visibility due to the sample is also expected as both figures were measured with different fibres (see text).

5. Discussion

CXD inversion algorithms require good quality data in order to converge appropriately. First, the signal-to-noise ratio must be optimized, with intensities at least 3 orders of magnitude bigger than the background counts. Achieving this condition with biological samples is difficult as they scatter weakly. Collagen Bragg peaks can be more than 10^6 times weaker than the transmitted beam, and this fact together with the limited dynamic range of the available detectors compromises the signal-to-noise ratio, therefore the ability to obtain a dark field image of the sample from an inversion algorithm. A way to improve the signal-to-noise ratio is to search for more ordered areas of the sample: if the measured volume is the same, the integrated diffracted intensity is conserved, but it is now distributed within a smaller Bragg peak. Collagen fibres within native tail tendon have a naturally high degree of axial order (with deviations of approximately 5º), although sample preparation and handling usually disturb the natural order of the fibres. For instance, Bragg peaks from our first coherent diffraction experiment on tail tendon samples [24] were 40º wide arcs. Since then we have improved our sample preparation protocol. Fibres are now kept wet during all the steps of the sample mounting and data acquisition processes. This has also increased the samples resistance to radiation damage by a factor of 5 approximately, as the liquid reduces the heat load on the fibers and delays the onset of the thermal denaturalization in collagen. It is also crucial to minimize, as much as possible, the time between tendon dissection and data recording, as the natural cross linkage of the fibres

degrades quickly within a few hours. Because of the small size of the fibres used, handling must be extremely careful in order to avoid any damage induced in the surface of the sample by the dissection tweezers during the mounting process. All these factors are particularly relevant in CXD experiments as both the sample and the beam used are much smaller than the ones in conventional SAXS, therefore the data are much more sensitive to small disorders induced in the sample. This new protocol was successfully applied in the experiments presented here, thus obtaining much narrower first order reflections from the collagen samples. These peaks are much less noisy that the ones we obtained in our first experiment [24], which will aid the phase retrieval process. We are developing also a new liquid cell for the samples with a design that minimizes the x-ray path within the buffer solution in order to decrease the incoherent scattering from the liquid.

Another requirement for easy convergence of the algorithms is a good degree of coherence in the beam; otherwise the speckle contrast is spoiled. The setup with a smaller coherence aperture (20 μm pinhole) at a shorter distance from the sample is more convenient for this aim. We would expect a better value of the speckle contrast if we had used even smaller apertures, or removed the mirrors of the beamline from the optical path, as slope errors and surface defects on the mirrors spoil the beam natural spatial coherence. It is also important to minimize the distance between the defining coherence aperture and the sample as well as to use a guard aperture at a suitable distance in order to remove the undesired parasitic scatter from the first aperture, hence "cleaning" the background counts. We found that the use of the second aperture increased the contrast of the patterns as we could exploit the dynamic range of the detector to its maximum.

We have shown that an undulator SAXS beamline can easily be modified for this type of study by the incorporation of two apertures for defining the coherence length. By this means, CXD data can be recorded and extra information from the sample can be extracted. Scanning SAXS gives the average orientation of fibres or crystallites within a matrix as well as the sample mean absorption with a resolution equivalent to the beam size. All this information is extracted from the magnitude of the scattered intensity. Iterative algorithms in CXD recover the transmission function of the sample both in amplitude and phase. This means that the reconstructed image would include extra information of the sample. For instance, the short range disorder in a fibre or crystallite matrix is encoded in the phase differences of the speckles within a Bragg peak. As a consequence, the reconstruction of the phase of the scattered wave from the sample contains information about the displacements from the ideal positions of the diffraction units, independently of the cause of these displacements. With this information it is possible to create strain or dislocation maps of the sample with extremely high resolution, as it has been already done in CXD for crystals [24]. This is particularly appealing for collagen tissues, as information concerning the mechanical properties of the tissue in the nanoscale could be directly obtained. Some scanning SAXS studies of these tissues give the average value of the orientation of the crystallites or fibres within the tissue with some tens of micron resolution. From these measurements an indirect estimate of some simple mechanical properties can be obtained. CXD could complement these studies with much higher resolution images. Moreover, when reconstructing coherent diffraction data from isolated Bragg peaks, the result will be a so-called dark field image of the sample, where the collagen matrix would be visible with contrast enhancement. These images will be very useful in bone studies when combined with conventional scanning SAXS data from where the distribution of apatite crystals can be extracted, to give a complete picture of the tissue.

6. Summary and outlook

We have discussed the improvements we have made in our sample preparation and experimental procedure in order to obtain high quality coherent diffraction data from collagen tissues. This is particularly relevant as only with high quality data, CXD reconstructions can be envisaged, hence all factors affecting the quality of data must be considered. Accurate sample handling protocols and the use of adequate coherence defining apertures are two relevant factors for increasing the signal-to-noise ratio of the measured Bragg peaks as well as their speckle contrast. Inversion of the obtained patterns

has still not been achieved, but is now more likely to be possible as CXD algorithms require high quality data. Eventually this will give dark field images of the tissues, with both amplitude and phase information from the sample. The reconstructed phase will be related to local disorder of the fibre positions on the short range, therefore will complement the information obtained by a conventional scanning and/or tomographic SAXS setup where the average orientation of the fibres within the tissue could be obtained. This will have consequences for micro and nanomechanics studies of collagen tissues, as high resolution information can be obtained without averaging large areas of the tissue.

The development of CXD methods applied to biological tissues is still at its initial stages; although we expect a rapid development of the techniques with the increasing availability of coherent sources (including the x-ray free electron lasers). This is a step towards the full imaging of biological tissues at the nanoscale.

Acknowledgments

We gratefully acknowledge the use of Diamond Light Source and the assistance of M. Malfois and C. Pizzey during the experiments. We also thank J. Rodenburg from University of Sheffield for fruitful discussions and T. Wess from University of Cardiff for providing some samples. The authors wish to acknowledge the support of EPSRC for funding this work through a Basic Technology Grant (EP/E034055/1) "Ultimate Microscopy: wavelength limited resolution without high quality lenses" and a Next Generation Facility development grant (EP/F020767/1) "Development of X-ray Ptychography at the Diamond Light Source.

References

[1] Roth S V, Burghammer M, Riekel C, Müller-Buschbaum P, Diethert A, Panagiotou P and Walter H 2003 *Appl. Phys. Lett* **82** 1935

[2] Schroer C G, Kuhlmann M, Roth S V, Gehrke R, Stribeck N, Almandarez Camarillo A and Lengeler B 2006 *Appl. Phys. Lett* **88** 164102

[3] Zizac I, Paris O, Roschger P, Bernstoff S, Amenitsch H, Klaushofer K and Fratzl P 2000 *J. Appl. Cryst.* **33** 820-823
Gupta H S, Seto J, Wagermaier W, Zaslansky P, Boesecke P and Fratzl P 2006 *Proc. Nat. Acad. Sci. USA* **47** 17741-17746
Gourrier A, Wagermaier W, Burghammer M, Lammie D, Gupta H S, Fratzl P, Riekel C, Wess T J and Paris P 2007 *J. Appl. Cryst.* **40** s78-82
Burger C, Zhou H, Wang H, Sics I, Hsiao B, Chu B, Graham L and Glimcher M J 2008 **95(4)** 1985-92

[4] Bunk O, Bech M, Jensen T H, Feidenhans'l R, Binderup T, Menzel A and Pfeiffer F 2009 *New Journal of Physics* **11** 123016
Boote C, Dennis S, Newton R H, Puri H and Meek K M 2003 *Invest. Ophthalmol. Vis. Sci.* **44** 2941-2948
Quantock A J, Boote C, Young R D, Hayes S, Tanioka H, Kawasaki S, Ohta N, Iida T, Yagi N, Kinoshita S and Meek K M 2007 *J. Appl. Cryst.* **40** s335-s340

[5] Riekel C, Madsen B, Knight D and Vollrath F 2000 *Biomacromolecules* **1(4)** 622-626

[6] Kennedy C J, Hiller J C**,** Lammie D, Drakopoulos M, Vest M, Cooper M, Adderley W P and Wess T J 2004 *NanoLetters* **8** 1373-1380
Hiller J C and Wess T J 2006 *J. Archeol. Sc.***33** 560-572

[7] Gerchberg R W and Saxton W O 1972 *Optik* **35** 237-246
Fienup J R 1982 *Appl. Opt.* **21(15)** 2758-2769
Elser V 2003 *J. Opt. Soc. Am. A* **20(1)** 40-55
Guizar-Sicairos M and Fienup J R 2008 *Opt.Express* **16(10)** 7264-7278

[8] Rodenburg J M and Faulkner H M L 2004 *Appl. Phys. Lett.* **85 4795-4797**
[9] Thibault P, Dierolf M, Menzel A, Bunk O, David C, Pfeiffer F 2008 *Science* **321** 379-382
[10] Maiden A M and Rodenburg J M 2009 *Ultramicroscopy* **109(10)** 1256-1262
[11] Sayre D 1952 *Acta Crystallogr.* **5(6)** 843
[12] Miao J, Charalambous P, Kirz J and Sayre D 1999 *Nature* **400** 342:344
Zuo J M, Vartanyants I, Gao M, Zhang R and Nagahara L A 2003 *Science* **300** 1419–1421
Williams G J, Pfeifer M A, Vartanyants I A and Robinson I K 2003 *Phys. Rev. Lett.* **90** 175501
Pfeifer M A, Williams G J, Vartanyants I A, Harder R and Robinson I K 2006 *Nature* **442** 63:66
[13] Miao J, Hodgson K O, Ishikawa T, Larabell C A, LeGros M A and Nishino Y 2003 *Proc. Natl. Acad. Sci. USA* **100** 110:112.
Shapiro D, Thibault P, Beetz T, Elser V, Howells M R, Jacobsen C, Kirz J, Lima E, Miao H, Nieman A M and Sayre D 2005 *Proc. Natl Acad. Sci. USA* **102** 15343:15346
Jiang H, *et al*. (2008) Nanoscale Imaging of Mineral Crystals inside Biological Composite Materials Using X-Ray Diffraction Microscopy *Phys. Rev. Lett*. 100, 38103
Song C, Jiang H, Mancuso A, Amirbekian B, Peng L, Sun R, Shah S S, Hong Zhou Z, Ishikawa T and Miao J 2008 *Phys. Rev. Lett.* **101** 158101
Nishino Y, Takahashi Y, Imamoto N, Ishikawa T and Maeshima K 2009 *Phys. Rev. Lett*. **102** 018101
[14] Bunk O, Dierolf M, Kynde S, Johnson I, Marti O and Pfeiffer F 2008 *Ultramicroscopy* **108(5)** 481-487
[15] Rodenburg J M, Hurst A C, Dobson B R, Pfeiffer F, Bunk O, David C, Jefimovs K and Johnson I 2007 *Phys. Rev. Lett*. **98** 034801
[16] Giewekemeyer K, Thibault P, Kalbfleisch S, Beerlink A, Kewish C M, Dierolf M, Pfeiffer F and Salditt T 2010 *Proc. Natl Acad. Sci. USA* **107** 529-534
[17] Hüe F, Rodenburg J M, Maiden J M and Midgley P A 2010 *submitted*
[18] Williams G J, Quiney H M, Dhal B B, Tran C Q, Nugent K A, Peele A G, Patterson D and De Jonge M D 2006 *Phys. Rev. Lett*. **97** 025506
[19] Abbey B, Nugent K A, Williams G J, Clark J, Peele A G, Pfeifer M A, De Jonge M and McNulty I 2008 *Nature Phys.* **4** 394-398
[20] Zhang F, Pedrini G and Olsen W 2006 *Opt. Lett.* **31(11)** 1633
[21] Zhang F, Pedrini G and Olsen W 2007 *Phys. Rev. A* **75** 043805
[22] Johnson I, Jefimovs K, Bunk O, David C, Dierolf M, Gray J, Renker D and Pfeiffer F 2008 *Phys. Rev. Lett*. **100** 155503
[23] Menzel A, Kewish C M, Dierolf M, Thibault P, Kraft P, Bunk O, Jefimovs K, David C and Pfeiffer F 2009 *J. of Phys: Conf Series* **186** 012054
[24] Berenguer de la Cuesta F, Wenger M P E, Bean R J, Bozec L, Horton M A and Robinson I K 2009 *Proc. Natl Acad. Sci. USA* **106** 15297-15301
[25] Rowe R W D 1985 *Conn. Tiss. Res.* **14(1)** 9-20
[26] Hulmes D J, Wess T J, Prockop D J and Fratzl P 1995 *Biophys. J*. **68** 1661:1670.
[27] Thompson B J and Wolf E 1957 *J. Opt. Soc. Am.* **47** 895